

Lindsay L. Loundagin¹

Human Performance Laboratory,
Faculty of Kinesiology,
University of Calgary,
2500 University Drive NW,
Calgary, AB T2N 1N4, Canada;
McCaig Institute for Bone and Joint Health,
University of Calgary,
Kinesiology Block B 221,
2500 University Drive NW,
Calgary, AB T2N 1N4, Canada
e-mail: lindsay.loundagin@ucalgary.ca

Tannin A. Schmidt

Human Performance Laboratory,
Faculty of Kinesiology,
University of Calgary,
2500 University Drive NW,
Calgary, AB T2N 1N4, Canada;
McCaig Institute for Bone and Joint Health,
University of Calgary,
2500 University Drive NW,
Calgary, AB T2N 1N4, Canada;
Schulich School of Engineering,
University of Calgary,
Kinesiology Block B 426,
2500 University Drive NW,
Calgary, AB T2N 1N4, Canada
e-mail: tschmidt@ucalgary.ca

W. Brent Edwards

Human Performance Laboratory,
Faculty of Kinesiology,
University of Calgary,
2500 University Drive NW,
Calgary, AB T2N 1N4, Canada;
McCaig Institute for Bone and Joint Health,
University of Calgary,
Kinesiology Block B 418,
2500 University Drive NW,
Calgary, AB T2N 1N4, Canada
e-mail: wbedward@ucalgary.ca

Mechanical Fatigue of Bovine Cortical Bone Using Ground Reaction Force Waveforms in Running

Stress fractures are a common overuse injury among runners associated with the mechanical fatigue of bone. Several in vivo biomechanical studies have investigated specific characteristics of the vertical ground reaction force (vGRF) in heel-toe running and have observed an association between increased loading rate during impact and individuals with a history of stress fracture. The purpose of this study was to examine the fatigue behavior of cortical bone using vGRF-like loading profiles, including those that had been decomposed into their respective impact and active phase components. Thirty-eight cylindrical cortical bone samples were extracted from bovine tibiae and femora. Hydrated samples were fatigue tested at room temperature in zero compression under load control using either a raw ($n = 10$), active ($n = 10$), low impact ($n = 10$), or high impact ($n = 8$) vGRF profile. The number of cycles to failure was quantified and the test was terminated if the sample survived 10^5 cycles. Fatigue life was significantly greater for both impact groups compared to the active ($p < 0.001$) and raw ($p < 0.001$) groups, with all low impact samples and 6 of 8 high impact samples surviving 10^5 cycles. The mean (\pm SD) number of cycles to failure for the active and raw groups was $12,133 \pm 11,704$ and $16,552 \pm 29,612$, respectively. The results suggest that loading rates associated with the impact phase of a typical vGRF in running have little influence on the mechanical fatigue behavior of bone relative to loading magnitude, warranting further investigation of the mechanism by which increased loading rates are associated with stress fracture.

[DOI: 10.1115/1.4038288]

Introduction

Mechanical fatigue is defined by the progressive damage and weakening of a material subjected to repetitive loads. Ultimately, this process may lead to catastrophic failure at stress magnitudes well below the material's monotonic strength [1]. Mechanical fatigue of load bearing bones is an inevitable consequence of physical activity owing to the continuous and repetitive nature of the mechanical loads experienced during walking and running. Over time, repetitive loading of the skeletal system causes microdamage accumulation that manifests as small cracks in the bony matrix. These microcracks reduce the overall quality of bone and lead to a reduction in apparent-level stiffness and an increase in mechanical strain with continued loading [2,3]. Without adequate bone remodeling and repair, the evolution and accumulation of microdamage may eventually lead to bone failure (i.e., fracture) [4]. Mechanical fatigue is believed to be the predominant etiology

of clinical stress fracture, which accounts for approximately 15% of all overuse injuries in running [5].

A typical vertical ground reaction force (vGRF) profile in heel-toe running illustrates the presence of two distinct peaks. The first of these peaks is preceded by a rapid increase in force attributable to a combination of a transient heel impact as well as nonimpact loads transmitted through the heel and distal foot [6]. This initial peak, commonly referred to as the "impact" peak [7], occurs within the first 15–50 ms after ground contact and ranges in magnitude from approximately 1.5 to 2.5 body weights [8,9]. Following the impact peak, the vGRF more slowly increases to a second peak occurring near midstance ranging in magnitude from approximately 2.5 to 3.0 body weights [8–10]. This latter peak is frequently referred to as the "active" peak [7] because it is associated with the center of mass fluctuations during running more directly under muscular control. The frequency band of the impact phase ranges from approximately 10 to 20 Hz, while major frequencies of the active phase are less than 10 Hz [6]. As the impact and active phases of running are superimposed in both the time- and frequency-domain during early stance, the decomposition of these two distinct events by simple time-series or spectral analyses is impractical. These two phases of the vGRF have been previously

¹Corresponding author.

Manuscript received March 10, 2017; final manuscript received October 20, 2017; published online January 17, 2018. Assoc. Editor: Kenneth Fischer.

separated with some accuracy using a cubic spline-based technique [11].

When treating the vGRF as a single time-series profile, several case-control studies have observed that runners with a history of stress fracture demonstrate higher rates of loading during the initial impact transient when compared to healthy matched controls [12–14], and these findings were verified through a meta-analysis on the topic [15]. More convincing evidence of the relationship between loading rate and stress fracture risk has come from a recent two-year prospective study of 249 female runners that reported higher impact loading rates in individuals that sought medical attention for running-related injury compared to those never injured [16]. These findings have led some to postulate that increased rates of loading are detrimental to skeletal health [15] and that stress fracture risk may be minimized by adopting running strategies that reduce or eliminate the impact transient in the vGRF [17,18], such as transitioning from a rear foot to a midfoot/forefoot strike pattern [19]. However, the mechanical properties of bone are only a weak function of loading rate (i.e., a ten-fold increase in strain rate increased elastic modulus by just 12% [20]), and much of the fatigue testing literature suggests that the number of cycles to failure actually increases with loading rate [21–23]. For example, a Weibull analysis accounting for stressed volume suggested that high frequency loading (30–125 Hz) extended fatigue life by a factor of approximately 1.33 when compared to low frequency loading (0.5–2 Hz) [24]. It is difficult to extrapolate these previous findings to in vivo biomechanical studies because they do not span the physiological range of loading frequencies associated with the vGRF in running.

The fatigue behavior of bone has frequently been examined ex vivo by cyclically loading small samples at various loading magnitudes and frequencies until failure [22,23,25]. However, the waveforms used for these tests are typically sinusoidal and not representative of the complex loading patterns experienced in vivo. The purpose of this study was to examine the fatigue behavior of cortical bone using vGRF-like loading profiles, including those that have been decomposed into their respective impact and active phase components. To this end, we have developed a novel experimental protocol for the fatigue testing of bone in order to determine, for the first time, whether the vGRF loading profiles associated with the impact or active phases of running are more influential to the fatigue life of bone. Based on findings from previous fatigue testing literature, we hypothesized that bone samples loaded with a low magnitude/high frequency waveform representing the impact phase of running would have a longer fatigue life than a higher magnitude/lower frequency waveform representing the active phase of running.

Methods

Cortical bone samples were machined from skeletally mature bovine tibiae and femora into a waisted “dog-bone” shape with circular cross section similar to other preparation protocols [23]; the sex, mass, health, and exact number of cows from which samples were harvested were unknown. The target dimensions of the samples were 35 mm in length and 7 mm in diameter, with a central gauge section 7 mm long and 5.25 mm wide (Table 1). The samples were kept wet with saline during preparation and stored at -30°C prior to testing. Samples were fitted with brass end caps to achieve gripping without damaging the bone. Prior to fatigue testing, apparent density was determined (i.e., wet weight divided by volume) and the initial elastic modulus was quantified with a bone-mounted extensometer (632.29F-30, MTS, Eden Prairie, MN) using a ramped compressive load of 220 N, corresponding to a stress of approximately 10.2 MPa. Mechanical testing was performed at room temperature on either a Bose Electroforce 3300 test frame (TA Instruments, New Castle, DE) or Instron Electropuls E3000 test frame (Instron, Norwood, MA). Differences in system compliance were not observed between these two

Table 1 Mean \pm SD for sample length, diameter, gauge diameter and the required force to produce a peak compressive force of 110 MPa for the active and raw group, 51.6 MPa for the low impact group and 82.7 MPa for the high impact group

	Sample length (mm)	Sample diameter (mm)	Gauge diameter (mm)	Force (N)
Raw	34.93 \pm 0.18	6.88 \pm 0.08	5.25 \pm 0.03	−2378.60 \pm 30.43
Active	35.10 \pm 0.09	6.81 \pm 0.09	5.23 \pm 0.05	−2362.43 \pm 47.56
Low impact	34.94 \pm 0.22	6.83 \pm 0.11	5.26 \pm 0.05	−1109.77 \pm 39.48
High impact	34.56 \pm 1.34	6.93 \pm 0.03	5.26 \pm 0.03	−1793.46 \pm 22.16

machines as indicated by crosshead displacements during modulus testing.

Thirty bone samples were harvested from eight tibiae and eight femora and randomly allocated to one of three different groups, and cyclically loaded in zero compression under force control using a raw ($n=10$), active ($n=10$), or low impact ($n=10$) vGRF profile (Fig. 1). An additional eight samples were harvested from two tibiae and two femora and assigned to a high impact vGRF profile and tested post hoc. The active profile was used to examine the effects of a relatively low loading rate and high loading magnitude, while the impact profiles were used to examine the effects of relatively high loading rates and low loading magnitudes. The raw vGRF profile allowed for the examination of both high loading rate and high loading magnitude. The raw vGRF profile was based on ensemble measurements from individual heel-toe running at 4.4 m/s [26]. Extraction of the impact and active phases of running was accomplished using a previously reported cubic spline routine [11]. Briefly, the active component of the vGRF was assumed to illustrate near-symmetric mass-spring behavior, with the initial 8 ms of the signal being the reverse of the final 8 ms of the signal. The spline was then relaxed (i.e., spline weights set to 0.0) from the initial 8 ms of the vGRF to twice the duration from heel strike to peak impact force. Spline weights after this region were set to 0.1, and forced through the final data point of the vGRF signal with a weight of 1.0. Application of the spline routine resulted in the active force profile; the low impact profile was obtained by subtracting the active profile from the raw vGRF curve. The additional high impact profile was created by scaling the extracted low impact profile to the initial peak of the raw vGRF profile. Custom waveforms were generated using either the WINTEST software (TA Instruments, New Castle, DE) for the Electroforce test frame to test the active, raw, and low impact profiles, or the WAVE MATRIX software (Instron, Norwood, MA) for the Electropuls test frame to test the high impact profile.

Peak forces of the vGRF profiles were scaled according to sample geometry (Table 1) to induce a peak axial compressive stress of 110 MPa for active and raw profiles. A peak stress of 110 MPa was chosen so that fatigue life measures could be compared to

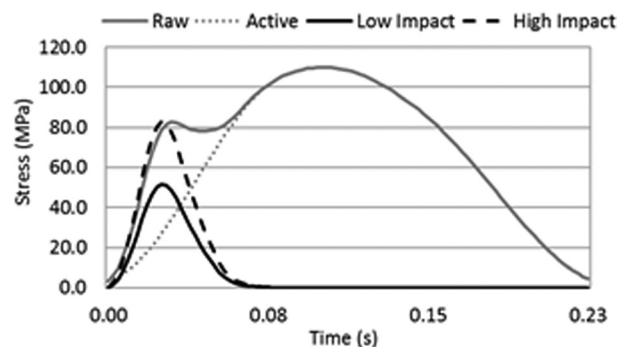


Fig. 1 Stress as a function of time for the raw, active, low impact, and high impact loading profiles

Table 2 Mean \pm SD for material properties, cycles to failure or run-out cycles, and the fraction of samples surviving 10^5 cycles in each group

	Elastic modulus (GPa)	Density (g/cm ³)	Cycles to failure/runout	Samples survived 10^5 cycles
Raw	19.8 \pm 1.6	2.02 \pm 0.03	16,552 \pm 29,612 ^a	1 of 10
Active	20.2 \pm 1.9	2.05 \pm 0.04	12,133 \pm 11,704 ^a	0 of 10
Low impact	20.9 \pm 1.8	1.98 \pm 0.08	100,000 \pm 0	10 of 10
High impact	21.6 \pm 2.2	1.88 \pm 0.33	89,081 \pm 25,575	6 of 8

^aSignificantly different from both impact groups ($p < 0.001$).

traditional zero-compression fatigue data from the literature [23]; this corresponded to an approximate strain range of 5500 $\mu\epsilon$, assuming an elastic modulus of 20 GPa (Table 2). The ratio of the peak force between the active and impact profiles resulted in a peak compressive stress of 51.6 MPa and 82.7 MPa for the low and high impact groups, respectively (Fig. 1). The duration for each individual curve, including the dwell time after both impact profiles, was 0.23 s, so that cycles/s were held constant at 4.35 Hz. This is not to be confused with the frequency of each waveform (as would be quantified by the Fourier transform of an individual curve), which was 4.35 Hz for the active profile and 11.75 Hz for the impact profiles; the raw profile was composed of both 4.35 and 11.75 Hz frequencies. The average strain rate was estimated for each loading profile as the slope of the region between 20% and 80% of the time to the first peak. The average strain rate for the active, low impact, high impact, and the initial portion of the raw curve was 0.05, 0.10, 0.16, and 0.14 s⁻¹, respectively.

Samples were cycled until failure, which was determined by catastrophic fracture (i.e., a rapid reduction in load) or if the sample survived 10^5 cycles the test was stopped and the bone was said to run out. A run out of 10^5 cycles has been used in previous fatigue studies of cortical bone [27,28], and in the present study, a test that ran out 10^5 cycles was completed within a reasonable time frame of 6.4 h. In the absence of a direct strain measurement, the steady-state creep rate of each sample was quantified as the slope of the minimum displacement (i.e., displacement at zero force) versus time curve between 20% and 80% of the fatigue life. The rate of stiffness degradation was also evaluated between 20% and 80% of the fatigue life as the change in secant stiffness relative to the initial stiffness per cycle. Secant stiffness was defined at each cycle as the ratio of peak force to peak displacement. Initial stiffness was calculated as the average stiffness from the first twenty cycles of steady-state loading. Statistical differences in material properties, creep rate, and stiffness degradation rate among groups were examined using a one-way analysis of variance. The Kruskal–Wallis nonparametric test, and post hoc pairwise comparisons adjusted for Bonferroni correction, was used to determine statistical differences in the fatigue life measurement between groups. The criterion alpha level was set to 0.05 for all statistical tests.

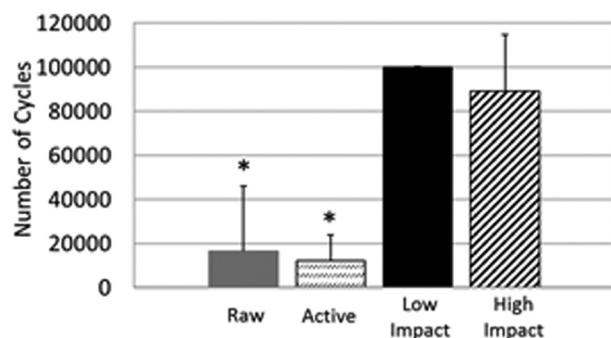


Fig. 2 Mean (\pm SD) number of loading cycles for the raw, active, low impact, and high impact. *Significantly different from both impact groups ($p < 0.001$).

Results

Samples allocated to each loading group did not differ significantly in terms of apparent density ($p = 0.145$) or initial elastic modulus ($p = 0.405$; Table 2). Fatigue life was significantly lower for the active group compared to both the high ($p = 0.006$) and low ($p < 0.001$) impact groups (Fig. 2). Similarly, the raw group had a significantly lower fatigue life compared to both the high ($p = 0.007$) and low ($p < 0.001$) impact groups. The mean number of cycles to failure (\pm SD) for the active and raw groups was 12,133 \pm 11,704 and 16,552 \pm 29,612, respectively (Table 2). Fatigue life was not significantly different between the active and raw groups ($p = 0.96$). All ten low impact samples and 6 of 8 high impact samples survived 10^5 cycles. The creep rate was significantly higher in the raw group compared to the high ($p = 0.010$) and low ($p = 0.011$) impact groups, but no difference was observed between the raw and active profiles ($p = 0.604$; Table 3). The rate of stiffness degradation per cycle was negligible prior to failure and no statistical differences were observed among the four loading groups ($p \geq 0.07$; Table 3).

Discussion

The purpose of this study was to examine the mechanical fatigue behavior of cortical bone using loading waveforms based on a typical heel-toe vGRF profile that was further decomposed into its respective impact and active phase components. Assuming that damage accumulation resulting from repetitive loading is the precursor to clinical stress fracture [29], the findings from this study challenge the general notion that higher loading rates associated with impact play a key role in the pathophysiology of stress fracture. This was demonstrated by a significantly lower fatigue life for samples in the active loading group when compared to the impact loading groups. Furthermore, the presence of an impact and higher initial loading rate in the raw vGRF profile did not significantly decrease fatigue life relative to the active profile even though both groups were loaded to the same peak stress. This, combined with the fact that 16 out of 18 samples from both impact groups ran out, provides strong evidence that the low magnitude/high frequency impact phase of running has little influence on the mechanical fatigue of bone as a material when compared to the higher magnitude/lower frequency active phase.

Previous fatigue studies of cortical bone have demonstrated a strong correlation between loading magnitude and fatigue life [25,30–32]. This relationship is often described by an inverse power law, indicating that small increases in stress will

Table 3 Mean \pm SD for creep rate and stiffness degradation rate for each group

	Creep rate ($\times 10^{-6}$ mm/s)	Stiffness degradation rate (N/mm/cycle)
Raw	25.98 \pm 26.53 ^a	−0.029 \pm .045
Active	17.01 \pm 15.76	−0.006 \pm .038
Low impact	1.21 \pm 1.25	−0.001 \pm .002
High impact	0.25 \pm 0.09	−0.009 \pm .032

^aSignificantly different from both impact groups ($p \leq 0.05$).

dramatically reduce the number of cycles to failure. Additionally, a positive relationship between loading frequency and fatigue life has been observed in both human and bovine cortical bone [21,22]. For example, a ten-fold increase in loading frequency was associated with a six-fold increase in the fatigue life of bovine bone loaded in zero tension [22]. Complimentary work from our lab examined the stress-life behavior of bovine cortical bone loaded in zero compression using sinusoidal waveforms at 3 and 9 Hz (see Supplemental Fig. S1, which is available under the “Supplemental Data” tab for this paper on the ASME Digital Collection.). These frequencies were similar to the physiologically relevant frequencies of 4.35–11.75 Hz explored in this study. A stepwise regression analysis of these data illustrated a combined $R^2 = 0.75$ ($p < 0.007$) with loading magnitude explaining 63% of the variance in fatigue life, and loading frequency explaining an additional 12% of the variance; both lower loading magnitude and higher loading frequency were associated with a longer fatigue life. Thus, according to existing research, we would only expect the active profile to have a shorter fatigue life than the impact profiles. Still, it is difficult to translate these previous findings utilizing sinusoidal waveforms to the physiological scenario because the effects of loading rate and loading frequency cannot be separated.

The raw vGRF profile is the superposition of the impact and active phases of running, which represent two distinct events that when decomposed, provided an impact profile (low impact) that was less than half that of the active profile (51.6 versus 110 MPa, respectively). To this effect, we also simulated and examined a high impact profile (82.7 MPa), which can be likened to the type of impact that would be observed during faster, or downhill, running [9,33]. The data in Supplemental Fig. S1, which is available under the “Supplemental Data” tab for this paper on the ASME Digital Collection, suggest that low impact samples would fail after approximately 10^6 loading cycles, whereas high impact samples would fail near 10^5 loading cycles. In other words, the peak loading magnitudes of the impact curves were either close to, or under, the endurance limit of bone. Rather than a study limitation, we see this as being further evidence of the importance of loading magnitude over loading rate as both impact profiles demonstrated a longer fatigue life than the active profile, despite having loading rates that were two-three times higher.

The tissue-loading environment of bone during active stance is comprised of both muscular and reaction forces, which, when combined, may induce stresses much higher than those predicted based on vGRF measurements. Indeed, in vivo strain gage measurements at the distal tibia in running would suggest that strains during active stance are some 2.5–8 times greater than that during impact [34–36], which would make the loading magnitude ratios investigated in this study conservative. Although it is possible that actual impact stresses may be higher than those examined herein, the skeptical individual need only examine Supplemental Fig. S1, which is available under the “Supplemental Data” tab for this paper on the ASME Digital Collection, as well as previous literature investigating different frequencies using sinusoidal waveforms [21,22,24]. These data clearly demonstrate that even when loading magnitude is held constant, the fatigue life of bone is greater at higher rates of loading. A more physiological representation of the influence of loading rate in human running is illustrated by comparing fatigue life data between active and raw samples in this study. These two profiles had similar peak magnitudes but different initial loading rates and no differences in fatigue life were observed. Conversely, a significantly different fatigue life was observed between the high impact and raw profiles. The high impact profile and initial impact peak of the raw profile had similar loading rates and magnitudes, suggesting that the decreased fatigue life of the raw group was due to the increased loading magnitude and longer loading duration associated with the active phase of the vGRF.

During fatigue testing, damage may accumulate as a function of loading duration (i.e., creep, or time-dependent damage), loading cycles (i.e., fatigue, or cycle-dependent damage), or both.

Cyclically, loading samples at different frequencies can elucidate this phenomenon. Zioupos et al. [22] cyclically loaded bovine and human bone in zero tension at 0.5 and 5 Hz. Samples loaded at 5 Hz tended to survive more cycles of loading, but no influence of loading frequency was observed as a function of time, suggesting creep-dominated failure. We observed similar time-dependent failure at different loading frequencies in zero compression (Supplemental Fig. S1, which is available under the “Supplemental Data” tab for this paper on the ASME Digital Collection.). In other words, the fatigue test could be considered a “continually interrupted creep” test, with the frequency of loading having no other effect than to influence the damage accumulated per cycle, but the total damage as a function of time remained the same. In addition to having a higher frequency, both impact profiles in the current study included a dwell period such that impact samples were only loaded 35% of the total cycle (0.08s), while the active and raw groups were loaded over the course of the entire cycle (0.23 s). These longer loading durations at higher loading magnitudes would be expected to make the active and raw groups more susceptible to creep damage and may help to explain the higher creep rate and reduced fatigue life of the active and raw groups when compared to the impact groups.

It is important to note that we are not attempting to suggest a lack of association between higher loading rates at impact and the risk of stress fracture. Indeed, both retrospective [12,13] and prospective [14,16] studies have demonstrated that such a relationship exists; though it should be mentioned these findings have predominantly come from a single lab. What these results do suggest is that loading rate, in and of itself, is not a causal mechanism in the pathogenesis of stress fracture. We hypothesize that the increased loading rates observed in the vGRF of those runners who develop a stress fracture may be indirectly related to the altered mechanics ultimately responsible for the resulting bone damage. The vGRF is an external force acting on the foot that represents the sum of all segmental accelerations [37]. As alluded to earlier, the vGRF is not necessarily representative of the internal multi-axial stress or strain state, of say the tibia, which is heavily determined by muscular loading [38]. In vivo strain gage studies have demonstrated increased strain magnitudes following muscular fatigue [39] and individuals with a history of stress fracture and have illustrated reduced muscular strength [40,41]. Perhaps, higher rates of loading at impact are simply a manifestation of a weakened or fatigued muscular state [42].

This study is limited to bovine cortical bone tested at room temperature in zero compression. These findings should be verified in human bone tested at physiological temperature, but we postulate this would simply modify, rather than confound, the effects observed herein such that relative differences between conditions would be similar and have no influence on the interpretation of the results. Additionally, ex vivo testing of small bone samples only describes the material response to experimental conditions and neglects factors that are present in vivo at the structural level, such as muscle forces that contribute to a more complex stress state or biological processes, including bone repair and adaptation. As a structure, long bones are generally loaded in bending [43], creating locations on either side of the neutral axis that solely fluctuate between zero tension and zero compression during each stride. Stress fractures are frequently observed on the compressive surface of long bones [44], making zero compression highly relevant; the fatigue life of cortical bone is slightly stronger in zero compression than zero tension by factor of 1.08 [24]. It is worth noting that Taylor et al. [23] cyclically loaded bovine cortical bone samples in zero compression using a 3 Hz sinusoidal waveform with a stress range of 100 MPa and observed a mean fatigue life of 15,060 cycles with 1–2 orders of magnitude variation in fatigue life. These results are similar to the mean fatigue life and variation for the active ($12,133 \pm 11,704$) and raw ($16,552 \pm 29,612$) loading profiles tested herein, for which no significant difference was observed. The large amount of variation (likely due to the inherent differences in bone microarchitecture

that were not investigated in this study) is a common finding in fatigue testing [24] and we do not anticipate that increasing our sample size would elucidate any further differences between active and raw groups. Although the difference in material properties among loading groups was not statistically significant, variation in the average density and elastic modulus was observed. We examined the influence this variation may have had on fatigue life measurements by normalizing the number of loading cycles to elastic modulus; however, significant differences between loading groups, and therefore the interpretation of our results, remained the same.

In summary, several in vivo biomechanical studies have investigated specific characteristics of the vGRF in heel-toe running and have observed an association between increased loading rate during impact and individuals with a history of stress fracture. In this study, we employed a novel testing paradigm to determine if the mechanical fatigue of bone at the material level was influenced more by loading profiles associated with the impact or active phase of running. The results from this study suggest that the loading rates associated with the impact phase of a typical vGRF in running have little influence on the mechanical fatigue behavior of bone relative to loading magnitude, warranting further investigation of the mechanisms by which increased loading rates are associated with bone stress injury.

Acknowledgment

Some of the mechanical testing were performed at Zymetrix (Calgary, AB, Canada).

Funding Data

- Natural Sciences and Engineering Research Council of Canada (Grant Nos. NSERC; RGPIN 01029-2015 and RTI 00013-2016).

References

- [1] Suresh, S., 1998, *Fatigue of Materials*, Cambridge University Press, New York.
- [2] Burr, D. B., Turner, C. H., Naick, P., Forwood, M. R., Ambrosius, W., Sayeed Hasan, M., and Pidaparti, R., 1998, "Does Microdamage Accumulation Affect the Mechanical Properties of Bone?," *J. Biomech.*, **31**(4), pp. 337–345.
- [3] Landrigan, M. D., Li, J., Turnbull, T. L., Burr, D. B., Niebur, G. L., and Roeder, R. K., 2011, "Contrast-Enhanced Micro-Computed Tomography of Fatigue Micro-damage Accumulation in Human Cortical Bone," *Bone*, **48**(3), pp. 443–450.
- [4] Burr, D., Milgrom, C., Boyd, R., Higgins, W., Robin, G., and Radin, E., 1991, "Experimental Stress Fractures of the Tibia Biological and Mechanical Aetiology in Rabbits," *J. Bone Jt. Surg., Br. Vol.*, **1**(1), pp. 370–375.
- [5] Brubaker, C., and James, S., 1974, "Injuries to Runners," *J. Sports Med.*, **2**(4), pp. 189–198.
- [6] Shorten, M., and Mientjes, M. I. V., 2011, "The 'Heel Impact' Force Peak During Running Is Neither 'Heel' nor 'Impact' and Does Not Quantify Shoe Cushioning Effects," *Footwear Sci.*, **3**(1), pp. 40–58.
- [7] Nigg, B., 1986, *Biomechanical Aspects of Running*, Human Kinetics, Champaign, IL.
- [8] Cavanagh, P. R., and LaFortune, M. A., 1980, "Ground Reaction Forces in Distance Running," *J. Biomech.*, **13**(5), pp. 397–406.
- [9] Munro, C., Miller, D., and Fuglevand, A., 1987, "Ground Reaction Forces in Running: A Reexamination," *J. Biomech.*, **20**(2), pp. 147–155.
- [10] Keller, T., Weisberger, A., Ray, J., Hassan, S., Shiavi, R., and Spengler, D., 1996, "Relationship Between Vertical Ground Reaction Force and Speed During Walking, Slow Jogging, and Running," *Clin. Biomech.*, **11**(5), pp. 253–259.
- [11] Derrick, T. R., Gillette, J. C., and Thomas, J. M., 2005, "Extraction of the Impact From Vertical Ground Reaction Force," 20th Congress of the International Society of Biomechanics (ISB), Cleveland, OH, July 31–Aug. 5, p. 773.
- [12] Milner, C. E., Ferber, R., Pollard, C. D., Hamill, J., and Davis, I. S., 2006, "Biomechanical Factors Associated With Tibial Stress Fracture in Female Runners," *Med. Sci. Sports Exercise*, **38**(2), pp. 323–328.
- [13] Ferber, R., Davis, I., Hamill, J., Pollard, C. D., and McKeown, K., 2002, "Kinetic Variables in Subjects With Previous Lower Extremity Stress Fractures," *Med. Sci. Sports Exercise*, **34**(5), p. S5.
- [14] Davis, I. S., Milner, C. E., and Hamill, J., 2004, "Does Increased Loading During Running Lead to Tibial Stress Fractures? A Prospective Study," *Med. Sci. Sports Exercise*, **36**(5), p. S58.

- [15] Zadpoor, A., and Nikooyan, A., 2011, "The Relationship Between Lower-Extremity Stress Fractures and the Ground Reaction Force: A Systematic Review," *Clin. Biomech.*, **26**(1), pp. 23–28.
- [16] Davis, I. S., Bowser, B. J., and Mullineaux, D. R., 2015, "Greater Vertical Impact Loading in Female Runners With Medically Diagnosed Injuries: A Prospective Investigation," *Br. J. Sports Med.*, **50**(14), pp. 887–892.
- [17] Crowell, H. P., and Davis, I. S., 2011, "Gait Retraining to Reduce Lower Extremity Loading in Runners," *Clin. Biomech.*, **26**(1), pp. 78–83.
- [18] Crowell, H. P., Milner, P. C. E., Hamill, J., and Davis, P. I. S., 2010, "Reducing Impact Loading During Running With the Use of Real-Time Visual Feedback," *J. Orthop. Sports Phys. Ther.*, **40**(4), pp. 206–213.
- [19] Lieberman, D. E., Venkadesan, M., Werbel, W. A., Daoud, A. I., Andrea, S. D., Davis, I. S., Ojiambo, R., Eni, M., and Pitsiladis, Y., 2010, "Foot Strike Patterns and Collision Forces in Habitually Barefoot Versus Shod Runners," *Nature*, **463**(28), pp. 531–535.
- [20] Carter, D. R., and Caler, W. E., 1983, "Cycle-Dependent and Time-Dependent Bone Fracture With Repeated Loading," *ASME J. Biomech. Eng.*, **105**(2), pp. 166–170.
- [21] Caler, W. E., and Carter, D. R., 1989, "Bone Creep-Fatigue Damage Accumulation," *J. Biomech.*, **22**(6–7), pp. 625–635.
- [22] Zioupos, P., Currey, J. D., and Casinos, A., 2001, "Tensile Fatigue in Bone: Are Cycles-, or Time to Failure, or Both, Important?," *J. Theor. Biol.*, **210**(3), pp. 389–399.
- [23] Taylor, D., Brien, F. O., Prina-mello, A., Ryan, C., Reilly, P. O., and Lee, T. C., 1999, "Compression Data on Bovine Bone Confirms That a 'Stressed Volume' Principle Explains the Variability of Fatigue Strength Results," *J. Biomech.*, **32**(11), pp. 1199–1203.
- [24] Taylor, D., 1998, "Fatigue of Bone and Bones: An Analysis Based on Stressed Volume," *J. Orthop. Res.*, **16**(2), pp. 163–169.
- [25] Carter, D. R., and Hayes, W. C., 1976, "Fatigue Life of Compact Bone-I: Effects of Stress Amplitude, Temperature and Density," *J. Biomech.*, **9**(1), pp. 27–34.
- [26] Edwards, W. B., Taylor, D., Rudolph, T. J., Gillette, J. C., and Derrick, T. R., 2009, "Effects of Stride Length and Running Mileage on a Probabilistic Stress Fracture Model," *Med. Sci. Sports Exercise*, **41**(12), pp. 2177–2184.
- [27] Vashishth, D., Tanner, K. E., and Bonfield, W., 2001, "Fatigue of Cortical Bone Under Combined Axial-Torsional Loading," *J. Orthop. Res.*, **19**(3), pp. 414–420.
- [28] George, W. T., and Vashishth, D., 2005, "Damage Mechanisms and Failure Modes of Cortical Bone Under Components of Physiological Loading," *J. Orthop. Res.*, **23**(5), pp. 1047–1053.
- [29] Warden, S. J., Burr, D. B., and Brukner, P. D., 2006, "Stress Fractures: Pathophysiology, Epidemiology, and Risk Factors," *Curr. Osteoporos. Rep.*, **4**(3), pp. 103–109.
- [30] Carter, D. R., Caler, W. E., Spengler, D. M., and Frankel, V. H., 1981, "Fatigue Behavior of Adult Cortical Bone: The Influence of Mean Strain and Strain Range," *Acta Orthop. Scand.*, **52**(5), pp. 481–490.
- [31] Swanson, S. A., Freeman, M. A., and Day, W. H., 1971, "The Fatigue Properties of Human Cortical Bone," *Med. Biol. Eng. Comput.*, **9**(1), pp. 23–32.
- [32] Gray, R., and Korbacher, G., 1974, "Compressive Fatigue Behavior of Bovine Compact Bone," *J. Biomech.*, **7**(3), pp. 287–292.
- [33] Gottschall, J. S., and Kram, R., 2005, "Ground Reaction Forces During Downhill and Uphill Running," *J. Biomech.*, **38**(3), pp. 445–452.
- [34] Carter, D. R., 1978, "Anisotropic Analysis of Strain Rosette Information From Cortical Bone," *J. Biomech.*, **11**(4), pp. 199–202.
- [35] Lanyon, L. E., Hampson, W. G., Goodship, A. E., and Shah, J. S., 1975, "Bone Deformation Recorded In Vivo From Strain Gauges Attached to the Human Tibial Shaft," *Acta Orthop. Scand.*, **46**(2), pp. 256–68.
- [36] Burr, D., Milgrom, C., Fyhrie, D., Forwood, M., Nyska, M., Finestone, A., Hoshaw, S., Saig, E., and Simkin, A., 1996, "In Vivo Measurement of Human Tibial Strains During Vigorous Activity," *Bone*, **18**(5), pp. 405–410.
- [37] Bobbert, M., Schamhardt, H., and Nigg, B., 1991, "Calculation of Vertical Ground Reaction Force Estimates During Running From Positional Data," *J. Biomech.*, **24**(12), pp. 1095–1105.
- [38] Derrick, T. R., Edwards, W. B., Fellin, R. E., and Seay, J. F., 2016, "An Integrative Modeling Approach for the Efficient Estimation of Cross Sectional Tibial Stresses During Locomotion," *J. Biomech.*, **49**(3), pp. 429–435.
- [39] Milgrom, C., Radeva-petrova, D. R., Finestone, A., Nyska, M., Mendelson, S., Benjuya, N., Simkin, A., and Burr, D., 2007, "The Effect of Muscle Fatigue on In Vivo Tibial Strains," *J. Biomech.*, **40**(4), pp. 845–850.
- [40] Beck, T. J., Ruff, C. B., Shaffer, R. A., Betsinger, K., Trone, D. W., and Brodine, S. K., 2000, "Stress Fracture in Military Recruits: Gender Differences in Muscle and Bone Susceptibility Factors," *Bone*, **27**(3), pp. 437–444.
- [41] Schnackenberg, K. E., Macdonald, H. M., Ferber, R., Wiley, J. P., and Boyd, S. K., 2011, "Bone Quality and Muscle Strength in Female Athletes With Lower Limb Stress Fractures," *Med. Sci. Sports Exercise*, **43**(11), pp. 2110–2119.
- [42] Clansey, A. C., Hanlon, M., Wallace, E. S., and Lake, M. J., 2012, "Effects of Fatigue on Running Mechanics Associated With Tibial Stress Fracture Risk," *Med. Sci. Sport. Exercise*, **44**(10), pp. 1917–1923.
- [43] Biewener, A., 1991, "Musculoskeletal Design in Relation to Body Size," *J. Biomech.*, **24**(1), pp. 19–29.
- [44] Boden, B. P., Osbahr, D. C., and Jimenez, C., 2001, "Low-Risk Stress Fractures," *Am. J. Sports Med.*, **29**(1), pp. 100–111.